Optimal Charge and Charge Response Determination through Conformational Space: Global Fitting Scheme for Representative Charge and Charge Response Kernel

Tateki Ishida*

Department of Theoretical and Computational Molecular Science, Institute for Molecular Science, Myodaiji, Okazaki 444-8585, Japan

Received: February 2, 2008; Revised Manuscript Received: April 30, 2008

We propose a global fitting scheme derived in the least-squares sense to estimate the optimal partial charge and charge response kernel (CRK), $\partial Q_a/\partial V_b$, with the data collected from conformational space sampling. We applied the global fitting method to the 1-butanol system and show the performance and accuracy of our global fitting procedure. In addition, we chose 1-pentanol as the test system for electronic structure change through conformational change and applied the global fitting method to it. From our study, it is indicated that intramolecular polarization can be influenced by intramolecular hydrogen bonding, and it is shown that our global fitting method can correspond to such a situation. Also, the global fitting procedure was tested on a large molecular system, 1-dodecanol. We show the results of the application of our fitting method for the system needed to sample large sets of data over a large conformational space. It is indicated that the nonlocality in intramolecular polarization in the alkyl chain sequence can be observed and that the large fluctuation of CRKs through nonbonded interactions such as intramolecular hydrogen bonding, as seen in the 1-pentanol case, can appear in common. The global fitting scheme we propose can be used for building molecular models considering polarization effects explicitly, even in the case of target systems that include many conformers.

I. Introduction

Among many factors that govern intra- and intermolecular interactions, electrostatic interactions can be the primary factor determining the properties of a target system in solution. Polarization effects through many-body interactions also are affected by the magnitude of electrostatic interactions. In addition, charge polarization through intramolecular interactions plays an important role. Therefore, it is necessary to consider these polarization effects in molecular modeling. As a modeling method that includes the above-mentioned polarization effects, we recentlyproposed and developed a charge response kernel (CRK) model employing an interaction site representation[1–4] that is the first-order response of instantaneous partial charges to the electrostatic potential change on each atomic site calculated by the ab initio method. Unlike conventional polarizable models,[5–17] the CRK model does not need empirical parameters and conditions. The CRK model is successful in elucidating the possibility of a nonempirical modeling strategy with the ability to reproduce molecular properties such as polarizability. Also, for the case of the linear variation of polarizability with the system size, which has been discussed in the literature,[17] the utility of the CRK model is promising in light of the description of polarization as the sum of local polarizabilities in the CRK model. These applications of the CRK model were performed for the situation that the molecular geometries were fixed (or optimized). When considering molecular flexibility, one should bear in mind that, corresponding to geometrical changes, charge response is altered through the modification of wave function. This means implicitly that the charges obtained from electrostatic potential fitting depend on conformation. Thus, molecular modeling with fixed charges is obviously not sufficient for the system that undergoes significant geometrical changes. Conventionally, atomic partial charges determined at a single geometry have been assumed to be valid for other geometries and have been used in most cases, instead of introducing changeable partial charges that depend on molecular conformations. However, in view of recent advances in computer power, one can expect to be able to search more extensive regions of conformational space and to sample and obtain data over a larger range of conformations. Therefore, it is considered that a method for determining partial charges based on data sampled through large conformational regions should be developed.

To date, some studies concerning the variation of atomic charges as a result of geometrical changes have been reported. Reynolds et al.[18] carried out a series of calculations of partial charges for different conformations so that the dipole moments for each conformer could be reproduced, where each charge was weighted by the relative population of the particular conformation as estimated from a Boltzmann distribution. They pointed out the importance of charge variation depending on molecular conformational change; however, their procedure was not described as a formalism of molecular modeling applicable for molecular dynamics simulations. Also, Dinur et al.[19] proposed a modeling methodology comprising atomic charges that depend on geometry. In their study, charge flux parameters were introduced as a measure for managing the geometry dependence of partial charges, and these parameters were determined by fitting ab initio calculation results for molecular dipole moments and their Cartesian derivatives at different molecular geometries. In their report, they stated that charge variation as a result of torsional motion was smaller in their model than that resulting from vibrational and bending motion. Thus, their approach does not seem to be appropriate for large conformational changes caused by torsional motion. In this study, a practical scheme for using collected geometry-dependent data including wide conformational changes is pursued. In

* E-mail: ishida@ims.ac.jp.

10.1021/jp800994q CCC: $40.75
Published on Web 07/09/2008

particular, an analysis procedure for fitting CRK data in a least-squares sense is shown.

Considering variations in the CRK that accompany geometrical changes of a molecule can expand the scope of model construction strategies. We can juxtapose the following two prescriptions. As a first strategy, we could redetermine the CRK depending on conformational change if the CRK were calculated at every conformational change. However, we can easily expect that, as the number of degrees of freedom increases, this will become very costly computationally. Therefore, the first method is not adequate for use in molecular dynamics simulations. As another prescription, if we could estimate the optimal response kernel as an "average" property, based on sampled data in conformational space, the CRK determined in such a way would be available as the CRK fitted to data collected from sampling space. For the purpose of molecular modeling in the simulation study, the second strategy seems to be promising, because, once the optimal CRK through conformational space has been estimated, the recalculation of the CRK is not needed. In the second method, a scheme is required to determine the optimal response kernel with the data collected from conformational sampling space. In the current study, we propose a procedure for computing optimal response kernel with calculation results at each point in the conformational sampling space as a *global fitting* in the least-squares sense, in a later section.

On the determination of the CRK with the global fitting through conformational space, it has to be determined that the approach in this study is applicable in various physical and chemical situations. We can consider the following two representative cases as examples: (a) a dramatic change in electronic structure resulting from intramolecular interactions and (b) molecular systems with large numbers of degrees of freedom where the combinations of variations of some degrees of freedom (in particular, correlation among torsional motions) could cause a marked conformational change. Both of these examples are explicitly related to the so-called nonbonded-interaction effect that is an important feature in the study of force fields for computer simulations.[20] Thus, it is essential to observe how nonbonded interactions could influence the geometry-dependent behavior of CRKs to assess the versatility of the modeling procedure with our global fitting scheme. Therefore, we chose following three systems as test cases and applied the global fitting procedure to each. As a small system, we selected 1-butanol to demonstrate the performance of our fitting scheme. For 1-butanol, detailed conformational study with vibrational spectroscopy and ab initio calculation has been reported,[21] so we can specify the representative conformational change path and it is appropriate for our purposes. Second, for the case of a change in electronic structure including intramolecular interactions, which implies nonbonded interactions, we chose 1-pentanol system to check the performance and versatility of our global fitting method and to show that the global fitting method can correspond to dramatic electronic structure changes. The study of the experimental detection of isomerization among conformers of 1-pentanol has been reported[22] and mentioned the effects of hydrogen bonding on the assignment of vibrational bands. As a large molecular system, 1-dodecanol was selected as a test example to observe the applicability of our global fitting scheme for obtaining optimal properties through huge conformational sampling space and the effect of nonbonded interaction on geometry-dependent CRKs. 1-Dodecanol is an isomer of *n*-dodecanol whose surface aggregation at the water−air interface has been investigated;,[23] thus this seems to be a good target from the viewpoint of molecular modeling of aggregate systems.

This article is organized as follows: Section II describes the details of the charge response kernel and the global fitting scheme with sampled data through conformational space in a least-squares sense. The fitting scheme is described in section III, along with computational details about the global fitting procedure, the density functional theory (DFT) calculations, and the derivation of partial charges. In section IV, the globally fitted results for the CRKs of 1-butanol, 1-pentanol, and 1-dodecanol are presented, and the performance and quantitative accuracy of our fitting procedure are discussed. Conclusions are presented in section V.

II. Theory

A. Charge Response Kernel. Here, the expression and definition of the charge response kernel are given. When we consider the change of electrostatic potential on the sites in the molecule, it is expected that the partial charges on the sites in the molecule could be altered due to the deformation of the electronic structure. Then, we can investigate the distribution of partial charges by fitting charges with respect to the electrostatic potential so that the fitted charges can reproduce the electrostatic field obtained with the wave function. Employing the interaction site representation, when the partial charge at atomic site a and the electrostatic potential at atomic site b are represented by Q_a and V_b, respectively, the CRK, K_{ab}, is defined as

$$K_{ab} = \frac{\partial Q_a}{\partial V_b} \tag{1}$$

With the wave function, the partial charges Q_a are determined by least-squares fitting to the electrostatic potentials generated by the electrons, and the nuclear charges of the molecule are evaluated at grid points distributed around the target molecule. The sum of the squared deviation between the quantum mechanical and classical electrostatic potentials on a grid point outside the molecule, L, is given by

$$L = \sum_n^{\text{grid}} w_n \left[-2 \sum_{i=1}^{N} \left\langle i \left| \frac{1}{|\mathbf{R}^{\text{grid}}(n) - \mathbf{r}|} \right| i \right\rangle + \sum_c^{\text{nuc}} \frac{Z_c}{|\mathbf{R}^{\text{grid}}(n) - \mathbf{R}^{\text{nuc}}(c)|} - \sum_a^{\text{sites}} \frac{Q_a}{|\mathbf{R}^{\text{grid}}(n) - \mathbf{R}(a)|} \right]^2 \tag{2}$$

where $\mathbf{R}^{\text{grid}}(n)$, $\mathbf{R}(a)$, $\mathbf{R}^{\text{nuc}}(c)$, and $\mathbf{r}$ represent the coordinates of grid point n, interaction site a, nucleus c, and the electron, respectively. i represents ith molecular orbital, and N is the total number of molecular orbitals. Z_c is the nuclear charge of atom c, and w_n represents the weighting factor for the grid n. It should be noted that interaction sites do not necessarily correspond to nuclear positions. Now, we show a general expression considering the minimization of L with the Lagrange multipliers κ and ξ for constraints on the total charge $Q = \sum_b^{\text{sites}} Q_b$ and the dipole moment μ, respectively

$$\frac{\partial}{\partial Q_a} \left\{ L - 2\kappa \left(\sum_b^{\text{sites}} Q_b - Q \right) - 2\xi \left[\sum_b^{\text{sites}} Q_b \mathbf{R}(b) - \mu \right] \right\} = 0 \tag{3}$$

Equation 3 leads to the equation for the set of charges $\{Q_a\}$

$$Q_a = \sum_b^{\text{sites}} [\mathbf{A}^{-1}]_{ab} \{ B_b + \kappa + \xi \cdot \mathbf{R}(b) \} \tag{4}$$

where $\mathbf{A}$ and $\mathbf{B}$ are given by

$$A_{ab} = \sum_{n}^{\text{grid}} w_n \frac{1}{|\mathbf{R}^{\text{grid}}(n) - \mathbf{R}(a)|} \frac{1}{|\mathbf{R}^{\text{grid}}(n) - \mathbf{R}(b)|} \quad (5)$$

$$B_a = \sum_{n}^{\text{grid}} w_n \left[-2 \sum_{i=1}^{N} \left\langle i \left| \frac{1}{|\mathbf{R}^{\text{grid}}(n) - \mathbf{r}|} \right| i \right\rangle + \sum_{c}^{\text{nuc}} \frac{Z_c}{|\mathbf{R}^{\text{grid}}(n) - \mathbf{R}^{\text{nuc}}(c)|} \right] \frac{1}{|\mathbf{R}^{\text{grid}}(n) - \mathbf{R}(a)|} \quad (6)$$

Next, the connection between the fitted partial charge and the system Hamiltonian with the perturbation consisting of the partial charge operator $\hat{Q}_a$ and the electrostatic potential V_a is explained.

In the derivation of the CRK, $K_{ab} = \partial Q_a / \partial V_b$, the system Hamiltonian including the perturbation is represented using the interaction site model as

$$\hat{H} = \hat{H}_0 + \sum_{a}^{\text{sites}} \hat{Q}_a V_a \quad (7)$$

where $\hat{H}_0$ is the zeroth-order Hamiltonian of the isolated molecule and the second term represents the perturbation of the Hamiltonian $\hat{H}_0$. The partial charge operator $\hat{Q}_a$ is defined by the least-squares fitting of the surrounding electrostatic potentials. The partial charge at site a, Q_a, is represented as

$$Q_a = \langle \Psi | \hat{Q}_a | \Psi \rangle \quad (8)$$

$$Q_a = \sum_{i}^{\text{elec}} \hat{q}_a(i) + Q_a^{\text{nuc}} \quad (9)$$

where Ψ denotes the wave function of the system. $\hat{q}_a(i)$ is the one-electron operator of the ith electron, and Q_a^{nuc} is the contribution from nuclear charges. Assuming that the Hellmann−Feynman theorem is fulfilled, Q_a and K_{ab} are given as the first and second derivatives, respectively, of the total energy E

$$Q_a = \frac{\partial E}{\partial V_a} \quad K_{ab} = \frac{\partial^2 E}{\partial V_a \partial V_b} \quad (10)$$

The CRK, K_{ab}, is rewritten in terms of the first derivative of the wave function Ψ^b with respect to V_b as follows

$$K_{ab} = \frac{\partial Q_a}{\partial V_b} = \langle \Psi^b | \hat{Q}_a | \Psi \rangle + \langle \Psi | \hat{Q}_a | \Psi^b \rangle \quad (11)$$

We denote the MO coefficient and its derivative with respect to V_b by C_{pi} and C_{pi}^{b}

$$\psi_i = \sum_{p}^{\text{AO}} \chi_p C_{pi} \quad \frac{\partial \psi_i}{\partial V_b} = \sum_{p}^{\text{AO}} \chi_p C_{pi}^b \quad (12)$$

where the subscripts p, q,... refer to atomic orbitals (AOs); the subscripts i, j,... refer to molecular orbitals (MOs); and C_{pi} and C_{pi}^{b} are related by the transformation matrix U^b

$$C_{qi}^b = \sum_{j}^{\text{MO}} C_{qj} U_{ji}^b \quad (13)$$

U^{b} is formulated by the linear equations, called the coupled-perturbed Hartree−Fock (CPHF) equations[1,24–26] in the HF case or the coupled-perturbed Kohn−Sham (CPKS) equations[27–31] in the case of DFT.

For the CPHF equation

$$(\varepsilon_l - \varepsilon_i) U_{li}^b + \sum_{j}^{\text{occ}} \sum_{k}^{\text{virt}} H_{likj}^{(\text{MO})} U_{kj}^b = -q_{b,li} \quad (14)$$

where i, j and k, l indicate the occupied and virtual MOs, respectively. $q_{b,li} = \langle l | \hat{q}_b | i \rangle$ is the matrix element of the one-electron partial charge operator $\hat{q}_b$ in the MO representation. This is related to the matrix element of $\hat{q}_b$ in the AO representation by

$$q_{b,il} = \sum_{r,s}^{(\text{AO})} q_{b,rs}^{(\text{AO})} C_{ri} C_{sl} \quad (15)$$

ε_i is the canonical orbital energy of the ith MO, and $H^{(\text{MO})}$ is the two-electron integral in the MO representation, defined as

$$H_{likj}^{(\text{MO})} = 4(li|kj) - (lk|ij) - (lj|ki) \quad (16)$$

In the case of the CPKS equation,[27–31] the two-electron integral is defined as

$$(\varepsilon_l^{\text{KS}} - \varepsilon_i^{\text{KS}}) U_{li}^b + \sum_{j}^{\text{occ}} \sum_{k}^{\text{virt}} H_{likj}^{\text{KS}} U_{kj}^b = -q_{b,li} \quad (17)$$

where H_{likj}^{KS} involves the derivative of the exchange-correlation functional

$$H_{likj}^{\text{KS}} = 4(li|kj) + 4\left(lk \left| \frac{\delta^2 E_{\text{xc}}[\rho]}{\delta\rho\delta\rho'} \right| ji \right) \quad (18)$$

where $(lk|\delta^2 E_{\text{xc}}[\rho]/\delta\rho\delta\rho'|ji) = \langle k|\delta V_{li}^{\text{xc}}[\rho]/\delta\rho|j\rangle$. The functional form of $\delta^2 E_{\text{xc}}[\rho]/\delta\rho\delta\rho'$ depends on the exchange-correlation functional $E_{\text{xc}}[\rho]$.

With the solution of eq 14 or eq 17, the CRK is represented as

$$K_{ab} = \sum_{i}^{\text{occ}} \sum_{l}^{\text{virt}} 4 q_{a,il} U_{li}^b \quad (19)$$

B. Global Fitting Scheme. ***1. Least-Squares Solution Adapted for Sampled Data through Conformational Space.*** In this section, we introduce the global fitting scheme with results sampled through conformational space. For global fitting in the least-squares sense with data sets, the sum of the squared difference between the quantum mechanical and classical electrostatic potentials on a grid of points external to the molecule, L_{global}, is defined as

$$L_{\text{global}} = \sum_{k}^{\text{conf}} \sum_{n}^{\text{grid}} w_{kn} \left[-2 \sum_{i=1}^{N} \left\langle i_{(k)} \left| \frac{1}{|\mathbf{R}^{\text{grid}}(k,n) - \mathbf{r}|} \right| i_{(k)} \right\rangle + \sum_{c}^{\text{nuc}} \frac{Z_c}{|\mathbf{R}^{\text{grid}}(k,n) - \mathbf{R}^{\text{nuc}}(k,c)|} - \sum_{a}^{\text{sites}} \frac{Q_a(k)}{|\mathbf{R}^{\text{grid}}(k,n) - \mathbf{R}(k,a)|} \right]^2 \quad (20)$$

where $\mathbf{R}^{\text{grid}}(k,n)$, $\mathbf{R}(k,a)$, $\mathbf{R}^{\text{nuc}}(k,c)$, and $\mathbf{r}$ represent the coordinates of grid point n at conformation k, interaction site a at conformation k, nucleus c (here, it is assumed that nuclear positions correspond to interaction sites) at conformation k, and the electron, respectively. $i_{(k)}$ represents the ith molecular orbital for conformer k. $Q_a(k)$ represents a partial charge at site a in conformation k. Z_c is the nuclear charge of atom c. w_{kn} represents the weighting factor for grid n at conformation k. Also, N means the total number of molecular orbitals.

In the case of no constraints at conformation k, the minimization of L_{global} through

$$\frac{\partial}{\partial Q_a(k)} L_{\text{global}} = 0 \tag{21}$$

results in the equation

$$\sum_b A_{ab}(k)\, Q_b(k) = B_a(k) \tag{22}$$

where $A_{ab}(k)$ and $B_a(k)$ are given by

$$A_{ab}(k) = \sum_n^{\text{grid}} w_{kn} \frac{1}{|\mathbf{R}^{\text{grid}}(k,n) - \mathbf{R}(k,a)|} \frac{1}{|\mathbf{R}^{\text{grid}}(k,n) - \mathbf{R}(k,b)|} \tag{23}$$

$$B_a(k) = \sum_n^{\text{grid}} w_{kn} \left[-2 \sum_{i=1}^{N} \left\langle i_{(k)} \left| \frac{1}{|\mathbf{R}^{\text{grid}}(k,n) - \mathbf{r}|} \right| i_{(k)} \right\rangle + \sum_c^{\text{nuc}} \frac{Z_c}{|\mathbf{R}^{\text{grid}}(k,n) - \mathbf{R}^{\text{nuc}}(k,c)|} \right] \frac{1}{|\mathbf{R}^{\text{grid}}(k,n) - \mathbf{R}(k,a)|} \tag{24}$$

With data sets and the constraint on the total charge in the global fitting, the equations for globally fitted charges Q_b are derived as

$$\sum_b A_{ab} Q_b = B_a + \kappa \tag{25}$$

where κ is the Lagrange multiplier to impose the constraint on the total of the globally fitted charges, $Q = \sum_b^{\text{sites}} Q_b$, and is given by

$$\kappa = \left(Q - \sum_a \sum_b A_{ab}^{-1} B_a \right) \Big/ \left(\sum_a \sum_b A_{ab}^{-1} \right) \tag{26}$$

A_{ab} and B_a are given by

$$A_{ab} = \sum_k A_{ab}(k) \quad B_a = \sum_k B_a(k) \tag{27}$$

2. Derivation of the Equation to Determine the Globally Fitted Charge Response Kernel. Next, we consider the representation of the derivative of globally fitted charge, Q_b, with respect to the electrostatic potential, V_c, on site c

$$K_{bc} = \frac{\partial Q_b}{\partial V_c} \tag{28}$$

From eqs 25–27, the equation to determine the globally fitted charge response kernel matrix can be derived as

$$\sum_b \sum_k A_{ab}(k) \frac{\partial Q_b}{\partial V_c} = \sum_k \frac{\partial B_a(k)}{\partial V_c} - \left[\sum_a \sum_b A_{ab}^{-1} \sum_k \frac{\partial B_a(k)}{\partial V_c} \right] \Big/ \left(\sum_a \sum_b A_{ab}^{-1} \right) \tag{29}$$

$$\frac{\partial B_a(k)}{\partial V_c} = \sum_b A_{ab}(k) \frac{\partial Q_b(k)}{\partial V_c} \tag{30}$$

III. Calculations

In this section, we explain the procedure and conditions of the calculations.

A. Geometry Optimization. Geometry optimization was carried out using the Gaussian 03 program.[32] For the calculations of 1-butanol and 1-pentanol, we employed the aug-cc-pVTZ[33] basis set and used diffuse functions only for oxygen. The geometric structures of all of the conformers were optimized with the B3LYP[34,35] functional. Optimization was carried out under C_1 symmetry except for one of 1-butanol conformers,

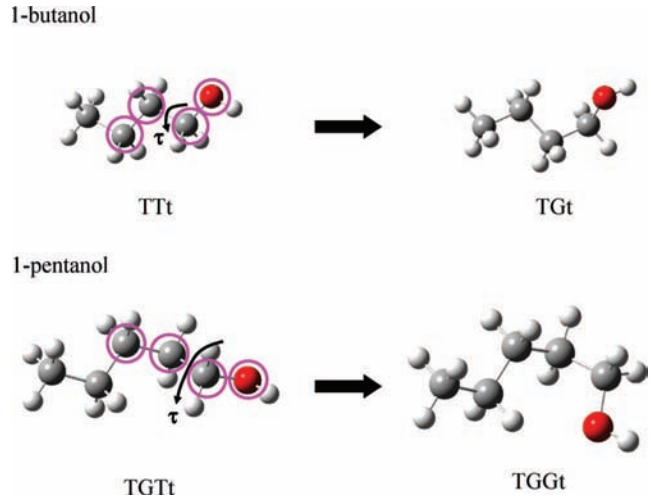

Figure 1. Conformers of 1-butanol, TTt and TGt, and 1-pentanol, TGTt and TGGt. (For abbreviations, see text.) τ = torsion angle defined by four encircled atoms (i.e., C—C—C—O).

TTt, for which the consecutive symbols denote the conformations about the CC—C—C—OH bond axes and T and t represent trans. The TTt conformer was optimized under C_s symmetry. For the optimization of 1-butanol, the geometries were prepared for seven conformers by changing the torsion angle C—C—C—O (see Figure 1) by 20° from 180° toward the TGt conformer (torsion angle τ = 64.69°). Then, the geometry optimization was carried out with only one torsion angle, C—C—C—O, fixed (see also Figure 1).

In the case of 1-pentanol, 10 geometries of conformers at every 30° from −180° toward the TGGt conformer (τ = 69.86°) were used. The geometry optimization was performed in the same way as for 1-butanol. Also, we prepared the 1-pentanol conformers and carried out geometry optimizations for later calculations. We considered the combination of choosing bonds (among the four bonds CC—C—C—C—OH, labeled 1−4, respectively) for counting conformers and took into account the situation that the rotation in the clockwise (+) or anticlockwise (−) direction is for the gauche (G or g) type, avoiding counting equivalent combinations. [For example, two sets of combinations of gauche type at the same bonds are (1, 2, 3, 4) = (G^+, G^+, G^+, g^+) and (G^-, G^-, G^-, g^-).] Hereafter, we omit the distinction between G and g in representing combinations. The number of conformers for the case of selecting only one bond from bonds 1−4 is 4. For choosing two bonds from bonds 1−4, the number of conformers is 12 [${}_4C_2 \times 2$, considering (+, +) and (+, −) pairs]. For selecting three bonds from bonds 1−4, the number of conformers is 16 [${}_4C_3 \times 4$, considering (+, +, +), (+, +, −), (+, −, +) and (−, +, +) pairs). The number of conformers for four bonds is 8 [(+, +, +, +), (+, +, +, −), (+, +, −, +), (+, −, +, +), (−, +, +, +), (+, +, −, −), (+, −, +, −) and (−, +, +, −)]. With one all-trans conformer, the total number of conformers is thus 41. We optimized all of the degrees of freedom and could obtain 40 optimized geometries except for the $G^-G^+G^-g^+$ conformer.

For 1-dodecanol, the Dunnning double-ζ plus polarization (DZP)[36] basis set was used. All conformers were optimized at the restricted Hartree−Fock (RHF) level. The sampling strategy in conformational space was as follows: Among a large number of combinations of selecting bonds around which rotations generate a variety of conformers of 1-dodecanol, we focused on the cases in which either one or two bonds were selected. As seen in Figure 2, each case was considered choosing one or

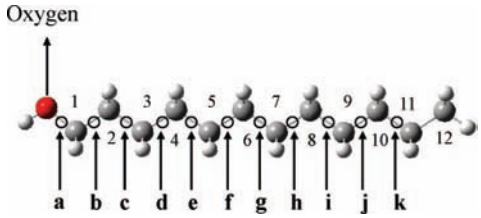

Figure 2. 1-Dodecanol: numbering on carbon atomic sites and denotations of bonds in chain sequence.

two bonds among 11 bonds $a-k$ in the figure. Considering rotation in positive (+) or negative (−) direction for the gauche (G) type and equivalent combinations as mentioned above in the 1-pentanol case, the number of conformers for the case of selecting two bonds is 110 [$55 = {}_{11}C_2$ for pairs with the same sign, e.g., (G^+, G^+), and 55 for pairs with opposite signs, e.g., (G^+, G^-)]. Also, there are 11 conformers for the case of choosing only one bond. Therefore, including one all-trans conformer, a total of 122 conformers were sampled and used for calculations. For each conformer selected by this method, geometry optimization was carried out under C_1 symmetry, except for the all-trans conformer, which was optimized under C_s symmetry.

B. Charge Response Kernel Calculation and Global Fitting. For all of the conformers, CRKs were calculated using the program code for the CRK calculation implemented in the GAMESS-UK package.[37,38] The CRK calculations for all cases were performed using the B3LYP hybrid functional. In the practical stage of CRK calculations, once the convergence in the electronic structure calculation was achieved and we obtained the wave function of the molecule, the following three steps were carried out: (1) We evaluated both **A** and **B** in eqs 5 and 6 and calculated the set of partial charges, $\{Q_a\}$, in the AO representation by using the results of the electronic structure calculations. (2) With the MO coefficients and eq 15, the partial charges in the AO representation were transformed to the MO representation to prepare the $q_{b,li}$ values on the right-hand side of eq 17. (3) To obtain the transformation matrix, **U**, eq 17 was solved with the CPKS iterative solver. After these three steps, finally, the CRK was computed with eq 19.

The grid-point distribution outside the molecule takes account of the molecular symmetry to make the fitted partial charges symmetry-adapted. The weighting factor w_{kn} in eq 20 for each grid point is commonly set to 1 in the current study. The grid-point distribution around each atomic nucleus was defined by the Lebedev grid-generating method[39,40] to avoid biasing grid points in certain angular directions around an atomic center. On the distribution of the grid points, first, a spherical shell of radius 1 au (= 0.53 Å) around each atom was generated, and grids were placed on the spherical shell by the Lebedev method, so that a total of 302 grid points were set on the unit sphere. Then, we increased the radius by 1 au and generated a new spherical shell with grids placed on it. This scheme was repeated until the distance from the center of the atom reached 20 au for each atom. The distributed grid points on each shell followed the point-group symmetry of the molecule. The grid points within a distance equal to the standard atomic van der Waals radius[41] on the envelopes were removed. Also, considering the Voronoi region[42] of each atom, the points that overlapped with grid points around different atomic sites were discarded. The total numbers of grid points for all of the conformers were ~11 000 for 1-butanol, ~12 000 for 1-pentanol, and ~20 000 for 1-dodecanol.

In least-squares fittings, we addressed the problem of ill-defined solutions, which cause unphysically large partial charges on the "buried" sites surrounded and shielded by neighboring sites.[2,3,43] Therefore, we employed the regulation method described in our previous study.[3] To regulate the ill-posed matrix problem of **A**, we minimized the square of the norm $\|\mathbf{AQ} - \mathbf{B}\|^2$ with an auxiliary penalty function (denoted as regulation method 2 in ref 3). The target function to be minimized, $S(\mathbf{Q})$, was set to

$$S(\mathbf{Q}) = \|\mathbf{AQ} - \mathbf{B}\|^2 + \lambda^2 p(\mathbf{Q}) \tag{31}$$

where $p(\mathbf{Q})$ is the penalty function and λ is a weight parameter for the penalty function. Here, $p(\mathbf{Q})$ is assumed to be a quadratic form of **Q** with unit matrix **I**

$$p(\mathbf{Q}) = \mathbf{Q}^{\mathrm{T}}\mathbf{IQ} \tag{32}$$

The minimization condition $\partial S(Q)/\partial Q = 0$ leads to the following solution of **Q**

$$\mathbf{Q} = (\mathbf{AA} + \lambda^2\mathbf{I})^{-1}\mathbf{AB} \tag{33}$$

The introduced regulation parameter λ was set equal to 0.05.[3]

The global fitting scheme was executed in the following three steps: (1) computation of the charge response kernel for each conformation using partial charges fitted without any constraints, that is, with $Q_a = \sum_b^{\mathrm{sites}}[\mathbf{A}^{-1}]_{ab}B_b$ from eq 4, (2) collection of data sets composed of matrix **A** and the charge response kernel matrix, and (3) global fitting of the charge response kernel for conformational change with the constraint on the total charge with eqs 29 and 30.

IV. Results and Discussion

In this section, we first show the globally fitted charges on some representative atomic sites of 1-butanol and the CRKs obtained by the global fitting and then discuss the performance and accuracy of the proposed global fitting scheme. Second, we report the calculated results of the case with the electronic structure change resulting from a conformational change for 1-pentanol as an example and discuss the robustness of the global fitting method. We also show the results of the global fitting procedure to a large molecular system, 1-dodecanol, and discuss the applicability of our fitting method for the system needed to collect large sets of data through conformational space.

A. Performance and Accuracy: 1-Butanol Case. The comparison of globally fitted charges with estimated partial charges at each conformer is displayed in Figure 3. As seen in Figure 3a,b, the partial charges on the carbon sites calculated by the global fitting were determined to be appropriately "averaged" values corresponding to the change of charges calculated for each conformer. On the other hand, the globally fitted charge on the oxygen site (Figure 3c) seems to be overestimated compared to the distribution of partial charges through the conformational change. However, the deviation of the globally fitted value from the charges determined for each conformer is about 0.02−0.03. Therefore, it is considered that the globally fitted charge on the oxygen site was also determined reasonably.

To verify that our global fitting procedure worked properly in a least-squares sense, we estimated the root mean square deviation (RMSD) of electrostatic potential between that obtained with fitted charges and that obtained with the wave function. In Figure 4a, we show the results of the RMSDs both with effective charges from the global fitting and with fitted charges at each conformer for 1-butanol. As expected, the

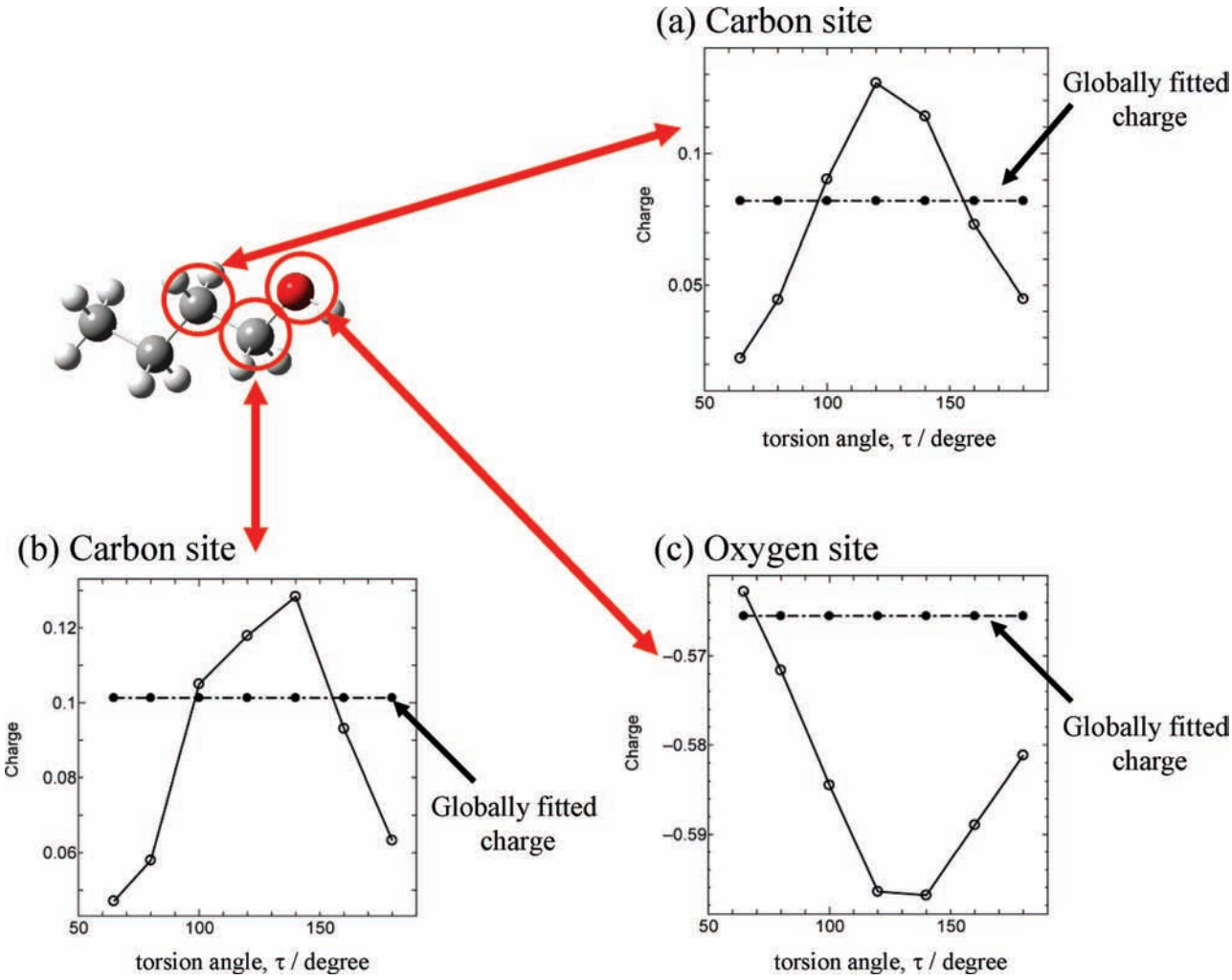

Figure 3. Globally fitted charges (●) in comparison with partial charges calculated at each conformer (○) for 1-butanol.

RMSDs with effective charges are relatively larger than those with charges calculated at each conformer. The difference between the two series of RMSDs is quite small at every point in the figure: less than 10^{-3}. Therefore, we consider that our global fitting procedure is able to give a good performance consistent with typical least-squares fitting methods.

To analyze the applicability and versatility of CRKs obtained through our global fitting scheme, we considered examining the accuracy of the CRKs obtained by evaluating the RMSDs of the electrostatic potential under the situation created by imposing a fluctuation in electrostatic potential to mimic the solution phase. The comparison of the CRKs obtained by the global fitting with the CRKs estimated at each conformer was carried out according to the following scheme: We considered the electrostatic potential fluctuation to evaluate partial charges

$$Q_a^{(\mathrm{local})} = Q_{a,\mathrm{gas}}^{(\mathrm{local})} + \sum_b K_{ab}^{(\mathrm{local})} \Delta V_b \tag{34}$$

$$Q_a^{(\mathrm{global})} = Q_{a,\mathrm{gas}}^{(\mathrm{global})} + \sum_b K_{ab}^{(\mathrm{global})} \Delta V_b \tag{35}$$

where $Q_{a,\mathrm{gas}}^{(\mathrm{local})}$ and $K_{ab}^{(\mathrm{local})}$ are partial charges and CRKs obtained in the gas-phase calculation by the least-squares fitting at each conformer and $Q_{a,\mathrm{gas}}^{(\mathrm{global})}$ and $K_{ab}^{(\mathrm{global})}$ are the corresponding quantities obtained by the global fitting procedure. ΔV_b represents electrostatic potential fluctuation imposed on the atomic site. To prepare the set $\{\Delta V_1, \Delta V_2, \ldots, \Delta V_n\}$, we took the reorganization energy due to polarization into account; that is, when the electrostatic potential fluctuation is imposed, the reorganization energy corresponding to polarization effects is represented using the CRK as

$$E = -\frac{1}{2}\sum_a \sum_b K_{ab} \Delta V_a \Delta V_b \tag{36}$$

In this case, the above representation can be rewritten by introducing the unitary matrix, U, composed of eigenvectors for eigenvalues, k, of the CRK matrix, K, as follows

$$E = -\frac{1}{2}\sum_c^{\mathrm{mode}} k_c \Delta \nu_c^2 \tag{37}$$

where $\Delta\nu = \Delta V U$. Thus, sets of $\{\Delta\nu_1, \Delta\nu_2, \ldots, \Delta\nu_n\}$ were generated assuming a Gaussian distribution with the standard deviation from the average, now $\Delta V = 0.0$, which corresponds to the situation in the gas phase, set to $E_{\mathrm{criterion}} = |-(1/2)k_c\nu_c^2| = 5.0$ kcal/mol, referring to the reported energy fluctuation in the ground state in the study with formaldehyde in aqueous solution.[44] Then, $\{\Delta\nu_1, \Delta\nu_2, \ldots, \Delta\nu_n\}$ were obtained using the equation $\Delta V = \Delta\nu U^{\dagger}$ (where $U^{\dagger}$ is the transposed matrix of U). With the generated sets of $\{\Delta\nu_1, \Delta\nu_2, \ldots, \Delta\nu_n\}$, we calculated the RMSDs of the electrostatic potential between those calculated with estimated charges using eqs 34 and 35 and those calculated with the wave function, including the set of externally imposed electrostatic potential fluctuations, $\{\Delta V_1, \Delta V_2, \ldots, \Delta V_n\}$.

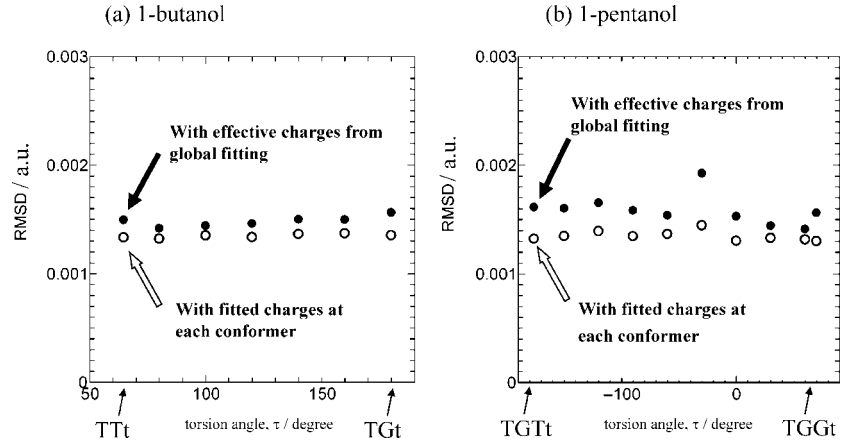

Figure 4. Comparison of RMSDs with effective charges obtained by global fitting and with partial charges fitted at each conformer: (a) 1-butanol and (b) 1-pentanol.

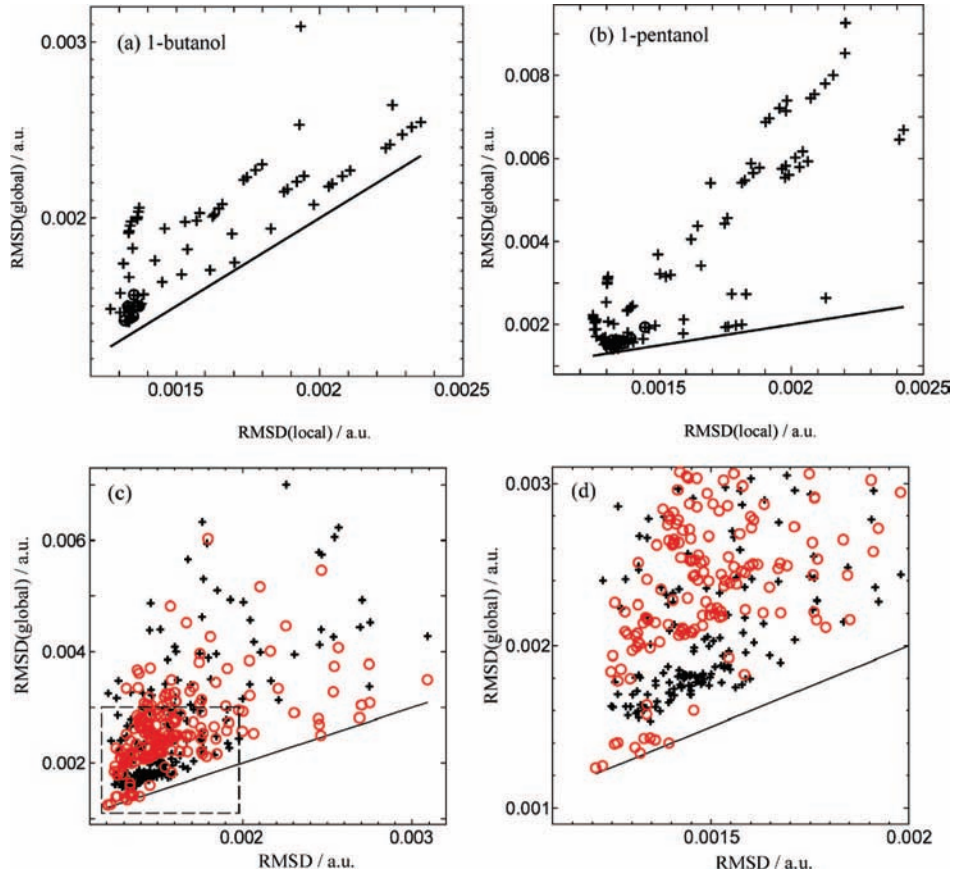

Figure 5. (a,b) Correlation between RMSD(local) and RMSD(global) with the correlation line of slope 1 to guide the eyes: (a) 1-butanol and (b) 1-pentanol. Pluses (+) are calculated results, and the gas-phase results in Figure 4 are mapped to circles (○). [See text for the definition of RMSD(local) and RMSD(global) in this figure.] (c,d) Correlation between RMSD(local) and RMSD(global) with the correlation line of slope 1 to guide the eyes: (c) 1-pentanol. Pluses (+) are calculated results, and circles (○) are with the fitted charges and CRK for all-trans 1-pentanol. (d) Magnification of the square region enclosed in the dashed line in c.

Here, we denote the RMSD obtained using $Q_a^{(\mathrm{local})}$ as RMSD(local) and that obtained using $Q_a^{(\mathrm{global})}$ as RMSD(global) for later discussion.

The results are shown in Figure 5a. For the 1-butanol case, we sampled 10 data points for each conformation of the 7 conformers of 1-butanol. In total, the calculation was carried out at 70 data points. In the figure, the RMSD data sets in the gas phase displayed in Figure 4 are included (shown as circles in Figure 5a). As seen in the figure, the data sets of RMSD(global) are larger than those of RMSD(local) (shown as pluses in Figure 5a). RMSD(local) and RMSD(global) are estimated to be very close to the distribution seen in Figure 4, and no problematic deviation in magnitude from the correlation line of slope 1 can be seen. Also, the data sets enclose the results in the gas phase. Therefore, these results indicate that the CRKs from the global fitting can reproduce well the properties with CRKs obtained at each conformer and, even in a situation such as a solution, we can expect that the globally fitted CRKs work well with sufficient accuracy in simulation studies. In summary, the proposed

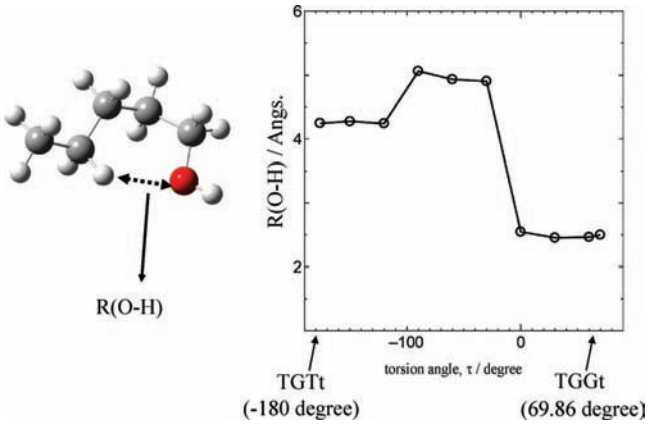

Figure 6. Definition of R(O···H) and its variation depending on torsion angle for 1-pentanol.

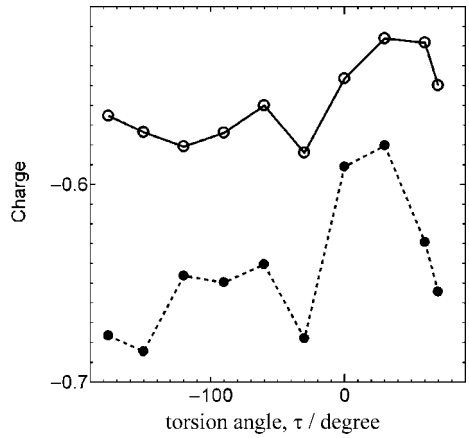

Figure 7. Comparison of the alteration of the fitted charges obtained between the procedure employed in the current study (○) and the Merz−Singh−Kollman procedure[45,46] (●).

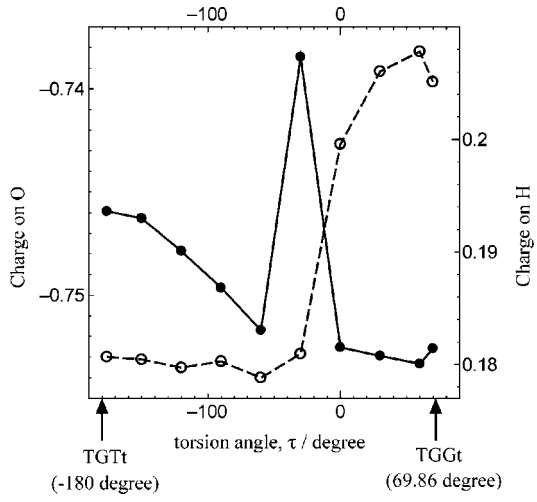

Figure 8. Comparison of the alteration of the charges on the oxygen and hydrogen sites in R(O···H) (see Figure 6) obtained by the NPA, corresponding to the conformational change from TGTt to TGGt in 1-pentanol: (●) charge on the oxygen site, (○) charge on the hydrogen site.

global fitting procedure can determine reasonable fitted values of charges on sites and CRKs, maintaining accuracy in a least-squares sense.

B. Robustness of the Global Fitting Scheme: 1-Pentanol Case. Compared to "normal" systems in which relatively large intramolecular interactions such as intramolecular hydrogen bonding do not occur, it is necessary to be cautious when treating a system that includes such effects, as it obviously accompanies a marked change of electronic structure. Corresponding to such cases, we needed to confirm that our global fitting method is applicable to systems that include intramolecular interaction, because checking that the global fitting can be adapted for large alterations of wave function is considered to warrant the robustness of our scheme. Here, as an example, we chose 1-pentanol, which exhibits an electronic structure change resulting from intramolecular interactions in conformational changes.

We considered four conformers of 1-pentanol, TTTt, GTTt, TGTt, and TGGt, where the letters denote the conformations about the CC—C—C—C—OH bond axes and T or t and G represent trans and gauche, respectively. Our ab initio calculations with the aug-cc-pVTZ basis set indicated that the TTTt conformer was lowest among the four conformers. The GTTt conformer was higher than TTTt by 0.9 kcal/mol, and TGTt was 0.09 kcal/mol higher than GTTt. Experimentally, the existence of the TTTt, GTTt, and TGTt conformers has been reported.[22] From TGTt to TGGt, the conformer was energetically raised by 0.7 kcal/mol. When we focus on the conformational change between TGTt and TGGt, the oxygen seems to be directed toward and to approach one of the hydrogen atoms in the alkyl groups, as seen in Figure 6. To investigate the degree to which the oxygen site can come close to the alkyl sequence following the OH group, we estimated the distance between the oxygen site and the hydrogen site for each conformer. It is shown in the figure that a rather large decrease (about 2.5 Å) in the distance occurs as the torsion angle changes between −30° and 0°. Judging from the data in the figure, we can expect a change in the partial charge on the oxygen atom site corresponding to the modification of the wave function as a result of the intramolecular interaction. We investigated the variation of the charge on the oxygen atom for each conformer in the transition from TGTt to TGGt. In Figure 7, the alteration of the partial charge on the oxygen atom estimated by our fitting procedure for each conformation is shown. As seen in the figure, a dip appears at $\tau = -30°$ in the variation. To verify that this result does not depend on fitting procedures, we examined the change of the partial charge with the Merz−Singh−Kollman fitting procedure.[45,46] The result is also displayed in the figure, for comparison with the result obtained by our fitting method. As is clearly shown in the figure, the results for the two fitting procedures show very similar profiles of the charge variation on the oxygen site. Therefore, we can conclude that the oscillating behavior in the variation of the partial charge around $\tau = -30°$ corresponds to the modification of the wave function accompanying the large change of the intramolecular distance, R(O···H), in Figure 6. In Figure 4b, the RMSDs with effective charges obtained by the global fitting are compared with those obtained using the partial charges fitted at each conformer. The gap between the two sets of RMSD data is small at each point except for the difference at −30°. This large gap can be attributed to the fluctuation of the partial charge on the oxygen site as discussed previously. Compared with the results at angles other than −30°, the gap seems to be larger, but even the deviation at −30° is less than $\sim 10^{-3}$. Therefore, our global fitting scheme works properly in a least-squares sense. Here, it is important to consider whether this large change of R(O···H) implies a dramatic change n wave function or not. We considered the change of partial charge on the oxygen and hydrogen sites (see Figure 6) employing natural population analysis (NPA). The results are shown in Figure 8. As seen in the figure, a decrease of the charge on the oxygen site was

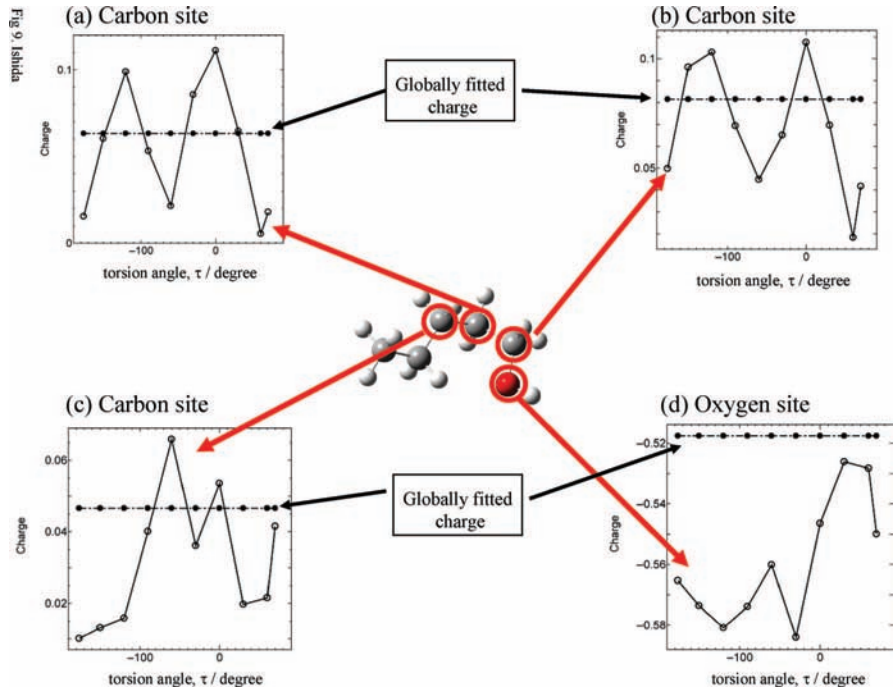

Figure 9. Comparison of globally fitted charges (●) with partial charges calculated at each conformer (○) for 1-pentanol.

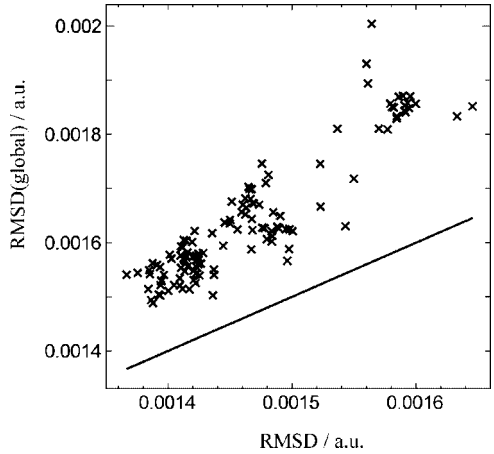

Figure 10. Correlation of RMSDs obtained by the global fitting and by the fitting at each conformer with a line of slope 1 to guide the eyes.

observed, although the magnitude of the decrease was not large and a small "bump" appeared. This is related to the appearance of the dip at $\tau = -30°$ in the RMSD data in Figure 4b as mentioned above. On the other hand, an increase of the charge on the hydrogen site was obtained. Thus, these data indicate a marked change in the wave function of 1-pentanol due to a large change in electronic structure such as charge transfer is less likely to be caused, but it is considered that the wave function of the system undergoes a slight modification as a result of intramolecular interactions.

Globally fitted charges are compared with partial charges estimated at each conformer in Figure 9. The partial charges on three carbon sites (Figure 9a−c) obtained by the global fitting are deduced to be nearly average values corresponding to the change of charges calculated for each conformer. As shown in the figure, the variation of the charges indicates oscillating behavior. The magnitude of the variation, however, is less than about 0.1, and it is considered that our global fitting procedure follows the variation and determines reasonably optimal values. In Figure 9d, the globally fitted charge on the oxygen site shows a difference from the distribution of partial charges through conformational change. However, the globally fitted value deviates from the charges determined for each conformer by only about 0.02−0.03. Therefore, our global fitting scheme reasonably determines the charge on the oxygen site as well. Regarding the fitted charge on the oxygen site, more details of the relation between the global fitting and the conformers included in the sampled is discussed in the later subsection on 1-dodecanol, which has features similar to those observed for 1-pentanol.

We examined the accuracy of the CRKs obtained by the global fitting with the same scheme as described in the previous subsection. In Figure 5b is shown a comparison of RMSD(local) with RMSD(global) for 1-pentanol. We sampled 10 data points for each conformer of the 10 conformations of 1-pentanol; thus, the RMSDs were calculated at a total of 100 points. The figure indicates that the magnitude of RMSD(global) is larger than that of RMSD(local) and that the data sets enclose the results in the gas phase. Therefore, it is considered that the CRKs from the global fitting have an accuracy almost equivalent to that of the CRKs obtained at each conformer and that the globally fitted CRKs are useful even in solution, as discussed in the case of 1-butanol. From the viewpoint of appropriately reasonable determination of CRKs, the globally fitted result is estimated to be close to the distribution of the direct result, following the effect of conformational change and intramolecular interactions.

Also, we investigated the accuracy of the CRKs obtained by the global fitting with all of the conformers of 1-pentanol. As described in section III, we prepared the optimized geometries for all possible 1-pentanol conformers. We sampled 5 data points for each optimized geometry of 40 conformations of 1-pentanol. Both RMSD(local) and RMSD(global) were calculated at a total of 200 points in the same way as in the previous subsection. In addition, we compared the results obtained with the estimated RMSD(local) and RMSD(global) values by using fitted charges and calculated CRKs for the all-trans conformer. We sampled 5 data points for each conformer except for the all-trans conformer; thus, the calculation was carried out at 195 points.

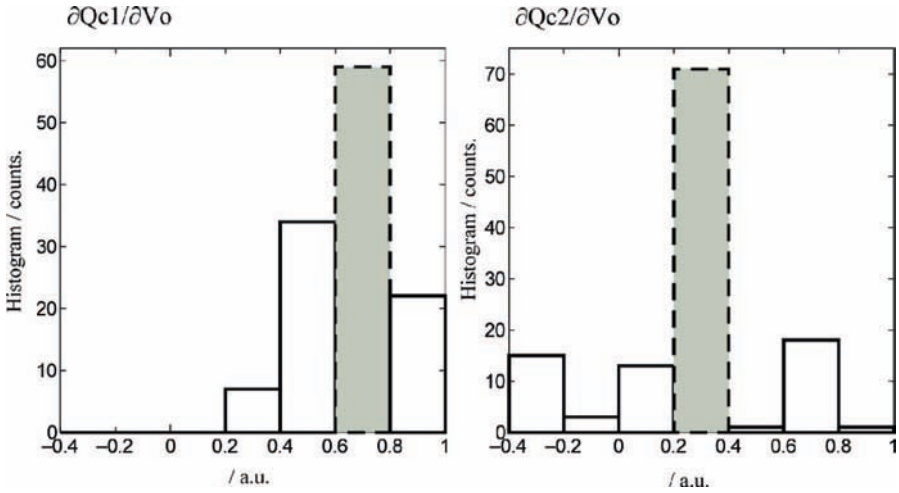

Figure 11. Histograms of the values of $\partial Q_{C1}/\partial V_O$ and $\partial Q_{C2}/\partial V_O$ by the windows with a 0.2 au bin. See text for explanation of strips with dark mesh.

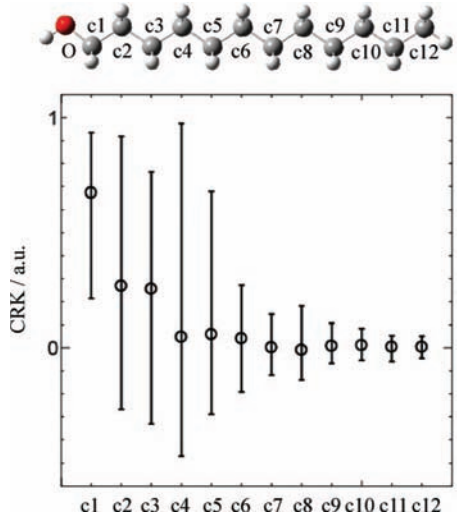

Figure 12. Molecular structure of 1-dodecanol with numberings on carbon sites and the range of $\partial Q_n/\partial V_O$ (n = C1−C12) values sampled for each conformer (as bars) with globally fitted results (○). Note that the bars in the figure do not represent error bars.

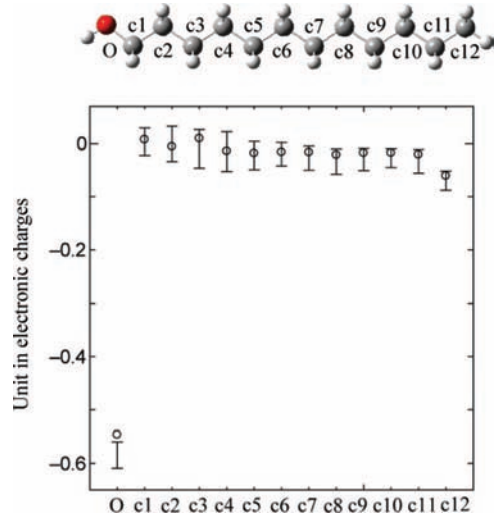

Figure 13. Ranges of fitted partial charges on carbon and oxygen sites. Circles (○) represent the values of effective charges from the global fitting. Note that the bars in the figure do not represent error bars.

In Figure 5c,d, comparisons of RMSD(local) with RMSD(global) are displayed. As seen in Figure 5c, the magnitude of RMSD(global)s is larger than that of RMSD(local), and about 75 % of the calculated points are included in the square with the dashed line in the figure. Figure 5d shows a magnification of the square region. From this figure, it can be seen that the magnitude of RMSD(global) at the most points obtained with the globally fitted CRK (shown as pluses in Figure 5c,d) is lower than that of RMSD(global) obtained with the CRK for all-trans 1-pentanol. Therefore, these results indicate that applying the globally fitted CRKs to the system that includes conformers can work better than using the CRK determined for one specific (or selected) conformer.

From the above discussion, we can conclude that the proposed global fitting method is applicable not only to typical systems that do not include specific interactions but also to systems that include intramolecular interactions and that it is useful for determining reasonable fitted values of the charges on sites and the CRKs for such a case.

C. Application to a Large System: 1-Dodecanol Case. In this subsection, we expand the range of target molecules and apply our global fitting method to the large molecular system 1-dodecanol, which includes a carbon chain consisting of 12 alkyl groups. In this case, we need to sample large sets of data for the global fitting through a vast conformational space. Therefore, it is our purpose here to investigate and discuss the applicability of the proposed global fitting scheme to sampling not in localized areas, but in extensive zones in a huge conformational space.

To check the robustness of our global fitting procedure throughout the sampled space, we calculated the RMSDs for both effective charges obtained by the global fitting and partial charges obtained by the usual fitting method for each conformer. Figure 10 shows the correlation between the RMSDs obtained by the global fitting and the usual fitting. The RMSDs with effective charges are larger than those with partial charges obtained at each conformer, as expected. As can seen in the figure, the deviation of the RMSDs obtained by the global fitting from those obtained by the fitting for each conformer is less than 10^{-3} for all of the sampled points. Therefore, it is considered that our global fitting method works well in a least-squares sense throughout a large conformational space.

Corresponding to conformational changes through sampled space, we can expect a change and a broad distribution of CRK matrix elements resulting from the modification of the wave

function. As a secondary check on the versatility of the proposed global fitting scheme, the CRK values determined by the global fitting were compared to those obtained by direct CRK calculation for each conformer. As we previously reported,[3] the nonlocal charge response to the perturbation at the O site is reduced through a few single (C—C or C—O) bonds following a hydroxyl group. Thus, it seems that the polarization at the C1 and C2 sites following the oxygen site can be influenced by both the polarization at the oxygen site and the molecular conformational change. Therefore, we chose the CRKs of three representative sites, namely, C1, C2, and O (see Figure 12), to observe the above-mentioned behavior of the CRKs. We sorted the matrix elements of the directly calculated CRKs, $\partial Q_{C1}/\partial V_O$ and $\partial Q_{C2}/\partial V_O$, with sampled data of 122 conformers into windows binned in 0.2-au intervals to generate histograms. The results are shown in Figure 11, where the gray shaded parts of the histograms enclosed in dashed lines are the most populated ranges in the distributions of $\partial Q_{C1}/\partial V_O$ and $\partial Q_{C2}/\partial V_O$. Also, each strip includes a globally fitted CRK value, as the fitted CRKs are 0.673 au for $\partial Q_{C1}/\partial V_O$ and 0.269 au for $\partial Q_{C2}/\partial V_O$, respectively. Therefore, the globally fitted CRKs were determined to be appropriate "mean" values for $\partial Q_{C1}/\partial V_O$ and $\partial Q_{C2}/\partial V_O$.

In addition, considering the nonlocality of the charge response we investigated,[3] the limited extent of the nonlocality through the alkyl chains can appear in large systems including alkyl chains, such as 1-dodecanol, and the profile of the nonlocality in intramolecular polarization is likely to be effective and *should be* covered even in the global fitting. In Figure 12, the range of $\partial Q_n/\partial V_O$ values (n = C1−C12) collected from the sampled data for each conformer and the globally fitted results are shown. The values of $\partial Q_{C1}/\partial V_O$ and $\partial Q_{C2}/\partial V_O$ indicate a larger range between upper and lower bounds than those on the $\partial Q_n/\partial V_O$ values (n = C6−C12). These behaviors are consistent with the reduction in the nonlocal charge response through the alkyl chain sequence: the polarization at a few carbon sites following the oxygen site of the hydroxy group at the end of chain sequence can be influenced, but the effect decreases as the carbon sites are farther from the oxygen site. However, the $\partial Q_n/\partial V_O$ values (n = C3−C5) show an irregularly large variation, in particular, of the upper bounds in the figure. We investigated the origin of this behavior, inspecting the molecular structures that gave rise to those upper bound data. Then, we found that the molecular geometries at the upper bound of $\partial Q_{C3}/\partial V_O$, $\partial Q_{C4}/\partial V_O$, and $\partial Q_{C5}/\partial V_O$ had in common much shorter R(O···H) contact distances (where H is attached to C4) than the other conformers. The value of the R(O···H) was about 2.5 Å on average. Our finding is similar to the case of 1-pentanol conformers in the previous subsection. Therefore, it is considered that irregular fluctuations in the upper bound data for $\partial Q_n/\partial V_O$ (n = C3−C5) correspond to the possibility that intramolecular polarization could be largely influenced by nonbonded interactions such as intramolecular hydrogen bonding. As a whole, the $\partial Q_n/\partial V_O$ values obtained by the global fitting procedure were determined to be among those for each conformer. These results indicate that the global fitting method can choose reasonable CRKs as fitted values that are appropriate for describing representative intramolecular polarization properties.

Figure 13 shows the results of the ranges of fitted partial charges on carbon and oxygen sites in the chain sequence calculated for each conformer, compared to effective charges obtained by the global fitting. Effective charges on carbon sites were determined to be within the range of data collected for each conformer. For the partial charge on the oxygen site, the globally fitted charge deviates from the range of partial charges fitted for each conformer. As previously discussed in the case of 1-pentanol, the global fitting tends to overestimate the partial charge on the oxygen site compared to the distribution of partial charges throughout conformers, and it behaves similarly also in the case of 1-dodecanol. At the present stage, it is considered that our global fitting procedure is applicable to the determination of the values of CRKs and effective charges considering the nonlocal profiles of CRKs in large systems with a warrant for the transferability of CRK modeling in the case of a system including many conformers.

V. Conclusions

In this article, we proposed a global fitting scheme derived in the least-squares sense. We applied the global fitting method first to the 1-butanol system and discussed the performance and accuracy of our global fitting procedure in relation to the globally fitted charges and CRKs. Second, we chose 1-pentanol as the test system for conformational changes and applied the global fitting method to it. From our investigation, it was shown that our global fitting method could estimate proper CRKs through conformational space. Also, the global fitting procedure was tested in a large molecular system, 1-dodecanol. We showed the results of the applicability of our fitting method for the systems that require sampling of large sets of data over a large conformational space. In addition, we found that nonlocality in the intramolecular polarization in the alkyl chain sequence could be observed, as in our previous study, and that large fluctuations in CRKs through nonbonded interactions such as intramolecular hydrogen bonding, as seen in the 1-pentanol case, could also appear.

In summary, the proposed global fitting scheme is applicable for building molecular models considering polarization effects explicitly even in the case that the target systems include many conformers. This procedure is promisingly for use in constructing polarizable models in molecular dynamics studies.

Acknowledgment. The author is grateful to Professor A. Morita for valuable and helpful comments. This work was supported by a Grant-in-Aid and the Next Generation Super Computing Project, Nanoscience Program, MEXT, Japan.

References and Notes

(1) Morita, A.; Kato, S. *J. Am. Chem. Soc.* **1997**, *119*, 4021.
(2) Morita, A.; Kato, S. *J. Phys. Chem. A* **2002**, *106*, 3909.
(3) Ishida, T.; Morita, A. *J. Chem. Phys.* **2006**, *125*, 074112.
(4) Morita, A.; Ishida, T. *Charge Response Kernel Theory based on Ab Initio and Density Functional Calculations*; Lecture Series on Computer and Computational Science; Brill Academic Publishers: Leiden, The Netherlands, 2005; Vol. 4, p 663.
(5) Mortier, W. J.; Ghosh, S. K.; Shankar, S. *J. Am. Chem. Soc.* **1986**, *108*, 4315.
(6) Rappe, A. K.; Goddard, W. A. *J. Phys. Chem.* **1991**, *95*, 3358.
(7) Rick, S.; Stuart, S. J.; Berne, B. J. *J. Chem. Phys.* **1994**, *101*, 6141.
(8) York, D. M.; Yang, W. *J. Chem. Phys.* **1996**, *104*, 159.
(9) Giese, T. J.; York, D. M. *J. Chem. Phys.* **2004**, *120*, 9903.
(10) Giese, T. J.; York, D. M. *J. Chem. Phys.* **2005**, *123*, 164108.
(11) Banks, J. L.; Kaminski, G. A.; Zhou, R.; Mainz, D. T.; Berne, B. J.; Friesner, R. A. *J. Chem. Phys.* **1999**, *110*, 741.
(12) Chelli, R.; Procacci, P. *J. Chem. Phys.* **2002**, *117*, 9175.
(13) Bultinck, P.; Langenaeker, W.; Lahorte, P.; De Proft, F.; Geerlings, P.; Waroquier, M.; Tollenaere, J. P. *J. Phys. Chem. A* **2002**, *106*, 7887.
(14) Bultinck, P.; Langenaeker, W.; Lahorte, P.; De Proft, F.; Geerlings, P.; Van Alsenoy, C.; Tollenaere, J. P. *J. Phys. Chem. A* **2002**, *106*, 7895.
(15) Chelli, R.; Procacci, P.; Righini, R.; Califano, S. *J. Chem. Phys.* **1999**, *111*, 8569.
(16) Nistor, R. A.; Polihronov, J. G.; Müser, M. H.; Mosey, N. J. *J. Chem. Phys.* **2006**, *125*, 094108.
(17) Warren, G. L.; Davis, J. E.; Patel, S. *J. Chem. Phys.* **2008**, *128*, 144110.

(18) Reynolds, C. A.; Essex, J. W.; Richards, W. G. *J. Am. Chem. Soc.* **1992**, *114*, 9075.
(19) Dinur, U.; Hagler, A. T. *J. Comput. Chem.* **1995**, *16*, 154.
(20) Leach, A. R. *Molecular Modeling—Principles and Applications*, 2nd ed.; Pearson Education Limited: Harlow, U.K., 2001.
(21) Ohno, K.; Yoshida, H.; Watanabe, H.; Fujita, T.; Matsuura, H. *J. Phys. Chem.* **1994**, *98*, 6924.
(22) Baonza, V. G.; Taravillo, M.; Cazoria, A.; Casado, S.; C′aceres, M. *J. Chem. Phys.* **2006**, *124*, 044508.
(23) Ravera, F.; Ferrari, M.; Santini, E.; Liggieri, L. *Adv. Colloid Interface Sci.* **2005**, *117*, 75.
(24) Gerratt, J.; Mills, I. M. *J. Chem. Phys.* **1968**, *49*, 1719.
(25) Pulay, P. *Analytical Derivative Techniques and the Calculation of Vibrational Spectra*; Modern Electronic Structure Theory Part II; World Scientific Publishing Co. Pte. Ltd.: Singapore, 1995; Vol. 2.
(26) Pople, J. A.; Krishnan, R.; Schlegel, H. B.; Binkley, J. S. *Int. J. Quantum Chem. Symp.* **1979**, *13*, 225.
(27) Handy, N. C.; Tozer, D. J.; Laming, G. J.; Murray, C. W.; Amos, R. D. *Isr. J. Chem.* **1993**, *33*, 331.
(28) Komornicki, A.; Fitzgerald, G. *J. Chem. Phys.* **1993**, *98*, 1398.
(29) Johnson, B. G.; Frisch, M. J. *J. Chem. Phys.* **1994**, *100*, 7429.
(30) Stratmann, R. E.; Burant, J. C.; Scuseria, G. E.; Frisch, M. J. *J. Chem. Phys.* **1997**, *106*, 10175.
(31) van Dam, H. *Second Derivatives of the Electronic Energy in Density Functional Theory*; Technical Report; CLRC Daresbury Laboratory: Warrington, U.K., 2001.
(32) Frisch, M. J.; Trucks, G. W.; Schlegel, H. B.; Scuseria, G. E.; Robb, M. A.; Cheeseman, J. R.; Montgomery, J. A., Jr.; Vreven, T.; Kudin, K. N.; Burant, J. C.; Millam, J. M.; Iyengar, S. S.; Tomasi, J.; Barone, V.; Mennucci, B.; Cossi, M.; Scalmani, G.; Rega, N.; Petersson, G. A.; Nakatsuji, H.; Hada, M.; Ehara, M.; Toyota, K.; Fukuda, R.; Hasegawa, J.; Ishida, M.; Nakajima, T.; Honda, Y.; Kitao, O.; Nakai, H.; Klene, M.; Li, X.; Knox, J. E.; Hratchian, H. P.; Cross, J. B.; Adamo, C.; Jaramillo, J.; Gomperts, R.; Stratmann, R. E.; Yazyev, O.; Austin, A. J.; Cammi, R.; Pomelli, C.; Ochterski, J. W.; Ayala, P. Y.; Morokuma, K.; Voth, G. A.; Salvador, P.; Dannenberg, J. J.; Zakrzewski, V. G.; Dapprich, S.; Daniels, A. D.; Strain, M. C.; Farkas, O.; Malick, D. K.; Rabuck, A. D.; Raghavachari, K.; Foresman, J. B.; Ortiz, J. V.; Cui, Q.; Baboul, A. G.; Clifford, S.; Cioslowski, J.; Stefanov, B. B.; Liu, G.; Liashenko, A.; Piskorz, P.; Komaromi, I.; Martin, R. L.; Fox, D. J.; Keith, T.; Al-Laham, M. A.; Peng, C. Y.; Nanayakkara, A.; Challacombe, M.; Gill, P. M. W.; Johnson, B.; Chen, W.; Wong, M. W.; Gonzalez, C.; Pople, J. A. *Gaussian 03*, revision C.01; Gaussian Inc.: Wallingford, CT, 2004.
(33) Woon, D. E.; Dunning, J. T. H. *J. Chem. Phys.* **1993**, *98*, 1358.
(34) Becke, A. D. *J. Chem. Phys.* **1993**, *98*, 5648.
(35) Lee, C.; Yang, W.; Parr, R. G. *Phys. Rev. B.* **1988**, *37*, 785.
(36) Dunning, J. T. H.; Hey, P. J. *Modern Electronic Structure Theory*; Plenum Press: New York, 1977.
(37) GAMESS-UK. is a package of ab initio programs written by Guest, M. F.; van Lenthe, J. H. ; Kendrick, J. ; Schoffel, K. ; Sherwood, P. with contributions from Amos, R. D. ; Buenker, R. J.; van Dam, H. J. J. ; Dupuis, M.; Handy, N. C. ; Hillier, I. H.; Knowles, P. J. ; Bonacic-Koutecky, V. ; von Niessen, W. ; Harrison, R. J. ; Rendell, A. P. ; Saunders, V. R. ; Stone, A. J. ; Tozer, D. J.; de Vries, A. H. The package is derived from the original GAMESS code by M. Dupuis, D. Spangler, and J. Wendoloski, NRCC Software Catalog, Vol. 1, Program No. QG01 (GAMESS), 1980.
(38) The initial DFT module within GAMESS-UK was developed by Dr. P. Young under the auspices of EPSRC's Collaborative Computational Project No. 1 (CCP1) (1995−1997). Subsequent developments have been undertaken by staff at the Daresbury Laboratory.
(39) Lebedev, V. I. *Zh. Vychisl. Mat. Mat. Fiz.* **1975**, *15*, 48.
(40) Lebedev, V. I. *Sib. Mat. Zh.* **1975**, *18*, 99.
(41) Bondi, A. *J. Phys. Chem.* **1964**, *68*, 441.
(42) Friesner, R. A. *J. Phys. Chem.* **1988**, *92*, 3091.
(43) Bayly, C. I.; Cieplak, P.; Cornell, W. D.; Kollman, P. A. *J. Phys. Chem.* **1993**, *97*, 10269.
(44) Naka, K.; Morita, A.; Kato, S. *J. Chem. Phys.* **1999**, *110*, 3484.
(45) Besler, B. H.; Merz, J. K. M.; Kollman, P. A. *J. Comput. Chem.* **1990**, *11*, 431.
(46) Singh, U. C.; Kollman, P. A. *J. Comput. Chem.* **1984**, *5*, 129.

JP800994Q